Volume 56(2): 111–123, 2008
Journal of Histochemistry & Cytochemistry
http://www.jhc.org

ARTICLE

Regeneration of Reinnervated Rat Soleus Muscle Is Accompanied by Fiber Transition Toward a Faster Phenotype

Luca Mendler, Sándor Pintér, Mónika Kiricsi, Zsuzsanna Baka, and László Dux

Institute of Biochemistry (LM,ZB,LD) and Department of Traumatology (SP), Faculty of General Medicine, and Department of Biochemistry (MK), University of Szeged, Szeged, Hungary

SUMMARY The functional recovery of skeletal muscles after peripheral nerve transection and microsurgical repair is generally incomplete. Several reinnervation abnormalities have been described even after nerve reconstruction surgery. Less is known, however, about the regenerative capacity of reinnervated muscles. Previously, we detected remarkable morphological and motor endplate alterations after inducing muscle necrosis and subsequent regeneration in the reinnervated rat soleus muscle. In the present study, we comparatively analyzed the morphometric properties of different fiber populations, as well as the expression pattern of myosin heavy chain isoforms at both immunohistochemical and mRNA levels in reinnervated versus reinnervated-regenerated muscles. A dramatic slow-to-fast fiber type transition was found in reinnervated soleus, and a further change toward the fast phenotype was observed in reinnervated-regenerated muscles. These findings suggest that the (fast) pattern of reinnervation plays a dominant role in the specification of fiber phenotype during regeneration, which can contribute to the long-lasting functional impairment of the reinnervated muscle. Moreover, because the fast II fibers (and selectively, a certain population of the fast IIB fibers) showed better recovery than did the slow type I fibers, the faster phenotype of the reinnervated-regenerated muscle seems to be actively maintained by selective yet undefined cues. **(J Histochem Cytochem 56:111–123, 2008)**

KEY WORDS
rat
soleus
reinnervation
notexin
regeneration
myosin heavy chain
fiber type transition

THE DIFFERENT TYPES of muscle fibers are highly dependent on their innervation pattern (Pette and Staron 1990; Pette and Vrbová 1992). Loss of innervation resulting from neuromuscular diseases or accidents leads to muscle inactivity, causing general morphological and physiological deterioration of the affected fibers (Gutmann and Zelena 1962; Borisov et al. 2001). Although myofibers are able to recover from denervation atrophy after the nerve–muscle contacts have been reestablished, muscle function, even after successful surgical repair, often fails to recover completely (Mackinnon and Dellon 1988; Hare et al. 1992; Kalliainen et al. 2002).

Reinnervation requires a fine interplay between nerve and muscle involving the regeneration of the injured nerve, the proper guidance of the regenerated axons to their target muscles, and muscle recovery from the denervation phenotype. Regarding nerve regeneration and guidance, several abnormalities have been described, such as axon loss after reconstructive surgery (Mackinnon et al. 1991; Lloyd et al. 2007), partial cross-reinnervation caused by foreign axons (Bodine-Fowler et al. 1997; Gramsbergen et al. 2000), or a high proportion of polyneurally innervated motor endplates (Ijkema-Paassen et al. 2002). In muscle recovery, microarray analysis has revealed that reinnervation may directly influence the molecular repertoire of myofibers by altering the expression of several factors involved in either neural regulation or fiber type determination (Zhou et al. 2006). It is known that the expression of slow myosin heavy chain (MHC) type I is absolutely dependent on slow-type nerve activity (Esser et al. 1993; Schiaffino and Reggiani 1996). In contrast, the fast-type innervation pattern maintains different fast isoforms (MHCIIA, IIX, and IIB). However, denervation or muscle inactivity has a similar effect on fast-isoform expression, inducing slow-to-fast shift with a concomitant increase in hybrid fibers in slow-type muscles (Ohira et al. 2006; Patterson et al. 2006). Cross-

Correspondence to: Luca Mendler MD, PhD, Institute of Biochemistry, Faculty of General Medicine, University of Szeged, Dóm tér 9, 6720 Szeged, Hungary. E-mail: luca@biochem.szote.u-szeged.hu

Received for publication July 24, 2007; accepted September 25, 2007 [DOI: 10.1369/jhc.7A7322.2007].

0022-1554/07/$3.30

reinnervation studies have also proved the plasticity of muscles by adapting the fiber phenotype to the properties of the newly innervating motoneurons (Vrbová et al. 1995).

Reinnervation has been shown to change the MHC composition of the target muscles at both mRNA and protein levels, although the extent and quality of alterations were highly dependent on the experimental procedure and the type of muscles examined (Bodine and Pierotti 1996; Huey and Bodine 1996; Sterne et al. 1997; Ijkema-Paassen et al. 2001,2005; Wang et al. 2002; Zhou et al. 2006). In contrast to mixed- or fast-type rat hindlimb muscles, which are characterized by an effective muscle recovery after reinnervation, we and others described long-lasting motor endplate and morphological abnormalities in the slow-type soleus after sciatic nerve transection and immediate repair by autologous graft (Ijkema-Paassen et al. 2001,2005; Pintér et al. 2003). Moreover, a slow-to-fast fiber type transition was also observed, which seemed to be stable even 60 weeks after nerve repair (Ijkema-Paassen et al. 2001,2005). Because satellite cells, the main source of postnatal muscle regeneration and growth (Bischoff 1994), have been described to be activated yet not fully differentiated in reinnervated rat muscles (Zhou et al. 2006), we hypothesized that the impairment of the muscle regenerative machinery may also be involved in the incomplete recovery of the soleus muscle.

To prove this hypothesis, we induced muscle necrosis and subsequent regeneration in the reinnervated soleus muscle 3 months after nerve repair by using notexin, the purified toxin of the Australian tiger snake, and followed the morphological changes during the course of muscle regeneration until day 28. Notexin destroys myofibers and motor endplate structures, leaving satellite cells and axons essentially intact (Harris et al. 1975,2000; Davis et al. 1991; Grubb et al. 1991). Motor endplates are reestablished on the surface of the regenerating muscle fibers in a few days, again building contacts to nerve terminals in intact innervation (Harris et al. 2000). This leads to the normalization of the nerve–muscle interaction and to an almost complete muscle recovery, regaining or even strengthening the innervation-dependent slow character of soleus by day 28 (Whalen et al. 1990; Sesodia and Cullen 1991, Lefaucheur and Sebille 1995, Zádor et al. 1996).

As opposed to normal regeneration, we found remarkable morphological alterations and motor endplate abnormalities throughout the regeneration process in reinnervated soleus (Pintér et al. 2003), which corroborated our hypothesis about the abnormalities of the regenerative machinery. To gain more insight into the underlying mechanisms, we performed in the present study morphometric, immunohistochemical, and mRNA analyses to investigate whether reinnervated soleus is able to reproduce its original fiber type pattern and size distribution after necrosis and regeneration. Here we show that the reinnervated fast-type soleus, unable to recover its original (slow) character, became even faster after muscle regeneration. This finding indicates that the (fast) pattern of reinnervation plays a dominant role in the specification of muscle phenotype during regeneration, which can also contribute to the long-lasting functional impairment of the reinnervated muscle.

Materials and Methods

Animals and Experimental Design

Adult male Wistar rats (270–340 g, $n=21$), obtained from the University of Szeged, Domaszék, Hungary, were used for the experiments. In the first group of animals (defined as reinnervated group, $n=7$), the left sciatic nerve was exposed at the proximal part of the thigh by splitting the gluteal muscle under intraperitoneal Nembutal anesthesia (0.5% Nembutal, 1 ml/100 g body weight). For denervation and immediate repair, a 12-mm nerve segment was resected and used as an autologous nerve graft in a reversed position to mimic a clinically relevant nerve reconstruction method (applying different peripheral nerves, such as sural nerve, to repair nerve injuries) and to avoid growth of axons through small side branches from the nerve graft (Mackinnon et al. 1991; Gramsbergen et al. 2000, Ijkema-Paassen et al. 2002; Pintér et al. 2003). The affected muscles first became denervated and atrophied, but after several weeks, reinnervation took place (Ijkema-Paassen et al. 2002; Pintér et al. 2003). Three months after the operation, the reinnervated soleus muscles and the contralateral untreated ones were removed. In the second group of rats (defined as reinnervated-regenerated group, $n=8$), sciatic nerve transection and immediate repair were carried out as described for the reinnervated group. However, 3 months after nerve repair, muscle necrosis was induced in the reinnervated soleus by intramuscular injection of 20 μg notexin as described previously (Zádor et al. 1996). On the 28th day of regeneration (4 months after nerve repair), the reinnervated-regenerated soleus muscles (and their contralateral counterparts) were removed. A third group of unoperated, age-matched rats (defined as normal group, 540–580 g, $n=6$) served as controls. All muscles were weighed, frozen in isopentane cooled by liquid nitrogen, and kept at −80C until further processing for morphological, immunohistochemical, and mRNA analysis. Animals were sacrificed with an overdose of Na-pentobarbital. All animal experiments were approved by the Institutional Animal Care and Use Committee at the University of Szeged in accordance with the U.S. National Institutes of Health guidelines for animal care.

Morphological and Morphometric Analysis of Muscles

For morphological analysis, cryostat sections of 15-μm thickness taken from the midbelly region of soleus muscles were stained with hematoxylin-eosin. In addition, motor endplates were visualized according to Tago's standard method (Tago et al. 1986) based on their acetylcholinesterase (AChE) activity. Total fiber number was counted in normal, reinnervated, and reinnervated-regenerated muscles analyzing the

whole cross section of each muscle (three muscles for each group) with the help of Olympus DP Soft software, Version 3.2. (Soft Imaging System GmbH; Münster, Germany). With the same software, mean fiber cross-sectional area (CSA) was calculated by measuring fiber CSA in at least three to four microscopic fields for each muscle (at least 300 fibers per muscle and three muscles for each group). Due to the high variability of fiber CSA in the different areas of muscle sections in both reinnervated and reinnervated-regenerated muscles, the microscopic fields were carefully taken for CSA analysis to represent the characteristic fiber populations and their proper ratio.

MHC Immunohistochemistry

For fiber type analysis, serial cryosections of 15-μm thickness of normal, reinnervated, or reinnervated-regenerated soleus muscles were subjected to MHC immunohistochemistry (Mendler et al. 1998). Sections were blocked in 5% non-fat milk powder/PBS, then incubated with mouse monoclonal antibodies BA-D5 (purified, 1:50), sc-71 (1:25), BF-F3 (1:10), and sc-75 (1:15) specific for MHCI (slow oxidative), MHCIIA (fast oxidative), MHCIIB (fast glycolytic), and MHCII (all types of fast fibers), respectively (DSMZ [National Resource Centre for Biological Material], Germany; Schiaffino et al. 1989). After incubation with the peroxidase-conjugated secondary antibody (rabbit anti-mouse; Dako, Denmark), immunocomplexes were visualized with diaminobenzidine staining with (sc-75) or without (BA-D5, sc-71, and BF-F3) nickel enhancement (in the presence of 0.15% nickel ammonium sulfate). Control sections were immunostained without primary antibodies. The number and proportion of different fiber types were calculated by counting total fiber number and fibers expressing different MHC isoforms with the help of Olympus DP Soft software, Version 3.2. (Soft Imaging System GmbH). Because of the lack of antibodies specific to MHCIIX, the number of pure (non-hybrid) IIX fibers was estimated according to the relative proportion of II, IIA, and IIB fibers (IIX = II − IIA − IIB); however, the calculation of IIX fiber subtypes (pure and hybrid) could not be established. The proportion of I/II hybrid fibers was estimated as follows: I/II (%) = type I (%) + type II (%) − 100 (%). The size (CSA) of slow MHCI– and fast MHCII–expressing fibers was measured on muscle sections immunostained with the MHCII-specific sc-75 antibody, as described above. In addition, the CSA of IIB fibers was analyzed on muscle sections stained with the MHCIIB-specific BF-F3 antibody.

RT-PCR Analysis

Total RNA was isolated according to the acid-guanidinium-thiocyanate-phenol-chloroform method (Chomczynski and Sacchi 1987), and reverse transcription was performed from normal (n=3), reinnervated (n=4), and reinnervated-regenerated (n=5) muscles as previously described (Mendler et al. 2000). cDNAs for MHCI, MHCIIA, MHCIIX, and MHCIIB were amplified at 94C for 1 min, at the appropriate annealing temperature for 1 min, and at 72C for 1 min using 2 U/tube Taq polymerase (Table 1) (Zádor et al. 1996; Jaschinski et al. 1998; Girgenrath et al. 2005). We applied two different sets of primers for MHCIIB amplification, both of which produced essentially the same amplification pattern, outlined in the Results section. For quantification, we used the 197 bp–long PCR fragment of MHCIIB (Jaschinski et al. 1998). After polyacrylamide gel electrophoresis, specific PCR products stained with ethidium bromide were quantified with the help of Quantity One software (Bio-Rad Laboratories; Hercules, CA). For the normalization of MHC mRNA levels, the transcript level of the glyceraldehyde-3-phosphate dehydrogenase (GAPDH) was proposed, which however, showed significant alterations in the different groups. Thus, total RNA gel electrophoresis was carried out, followed by the quantification of 28S rRNA, which served as an appropriate internal control because of its relative stability in the examined muscles.

Statistical Analysis

Each group of rats, for either protein or mRNA analysis, consisted of three to five animals. Data are reported as mean ± SEM. Statistical differences between groups were analyzed using either unpaired t-tests or one-way ANOVA, followed by a Newman-Keuls posttest (GraphPad Software, Inc.; San Diego, CA). For CSA measurements, 300–1200-fiber CSAs were summarized from three muscles per animal group. If fiber size distribution data violated the assumptions of normality and variance, they were also compared using a Kruskal-Wallis one-way ANOVA test, and differences between individual groups were analyzed by Dunn's posttest.

Table 1 PCR conditions of different MHC isoforms and GAPDH

Amplified product	Primer sequence (5′–3′) (forward and reverse)	Fragment size (bp)	Cycle number	Temperature (C)	Reference
MHCI	acagaggaagacaggaagaacctac gggcttcacaggcatccttag	288	17	94-60-72	Jaschinski et al. 1998
MHCIIA	tatcctcaggcttcaagatttg taaatagaatcacatggggaca	309	18	94-55-72	Jaschinski et al. 1998
MHCIIX	cgcgaggttcacaccaaa tcccaaagtcgtaagtacaaaatgg	121	18	94-58-72	Jaschinski et al. 1998
MHCIIB	ctgaggaacaatccaacgtc ttgtgtgatttcttctgtcacct	197	20	94-55-72	Jaschinski et al. 1998
	gaagagccgagaggttcacac caggacagtgacaaagaacgtc	108	20	94-55-72	Girgenrath et al. 2005
GAPDH	tcctgcaccaccaactgcttagcc tagcccaggatgccctttagtggg	378	16	94-60-72	Zádor et al. 1996

Results

Muscle Weight, Fiber Number, and Mean Fiber CSA

Because of nerve transection and immediate repair by graft, the sciatic nerve first degenerated, accompanied by the simultaneous transient denervation and inactivity of hindlimb muscles. However, the repaired nerve started to regenerate, reinnervating the hindlimb muscles ~7 weeks after the operation (Ijkema-Paassen et al. 2002). In accordance with other morphological, motor endplate, and functional studies of sciatic nerve recovery (Hare et al. 1992; Sterne et al. 1997; Ijkema-Paassen et al. 2001,2002), we found that by 3–4 months after microsurgery, the weight and morphology of reinnervated soleus muscles reached a near-optimal status and improved only slightly afterwards (Pintér et al. 2003). At this stage (3 months), the weight of the affected soleus was ~72% that of its contralateral counterpart (Figure 1A, reinnervated group), and both total fiber number and mean CSA of reinnervated soleus were significantly lower than those of normal soleus (Figures 1B and 1C, respectively), showing a partial recovery of reinnervated soleus from the denervation phenotype. Upon inducing muscle necrosis and subsequent regeneration, the muscle weight of reinnervated-regenerated muscles (on day 28 of regeneration) tended to further decrease (from 72% to 65%) (Figure 1A, reinnervated-regenerated group), and even after 35 days of regeneration, it did not increase considerably (data not shown, Pintér et al. 2003). Similarly, a further significant drop was observed in the total fiber number of reinnervated-regenerated muscle (Figure 1B). Yet, the mean fiber CSA increased when compared with reinnervated muscles (Figure 1C). According to our previous findings, normally innervated soleus muscles undergo a near-complete regeneration, reaching the total fiber number and 70–80% of the mean fiber CSA by day 28 (Zádor et al. 1996 and unpublished data). Thus, our morphometric data indicate that there is a partial impairment of the regeneration process (involving mainly muscle weight and fiber number), because certain quantitative properties (i.e., fiber CSA) did not change the same way in reinnervated-regenerated soleus muscles when compared with reinnervated ones. However, the mean fiber CSA of all fiber types does not give information about the potentially altered recovery of different fiber populations (i.e., MHCI- versus MHCII- versus MHCIIB-expressing fibers) in reinnervated-regenerated muscle.

Muscle and Motor Endplate Morphology

As we revealed earlier in accordance with the literature (Ijkema-Paassen et al. 2001; Pintér et al. 2003), reinnervated soleus muscle became generally atrophied, but the extent of atrophy was variable in different fibers and fiber groups (compare Figures 2A and 2B). In addition, the accumulation of connective tissue was a characteristic feature of these muscles (Figure 2B, asterisk). This finding could also explain why the muscle weight of reinnervated soleus was not as much decreased (compared with contralateral) as expected on the basis of the remarkable decrease in total fiber number and mean fiber CSA in our experiments. After inducing muscle necrosis and regeneration, we found an even higher variability in fiber size compared with reinnervated muscles (Figure 2C). In addition, more than 80% of central-localized nuclei were counted, a parameter significantly different from that in normal regeneration (Figure 2C, arrows). The amount of connective tissue was also increased (Figure 2C, asterisk), and its accumulation pattern around single fibers was a novel finding distinct from that observed during reinnervation (compare Figures 2B and 2C) and normal

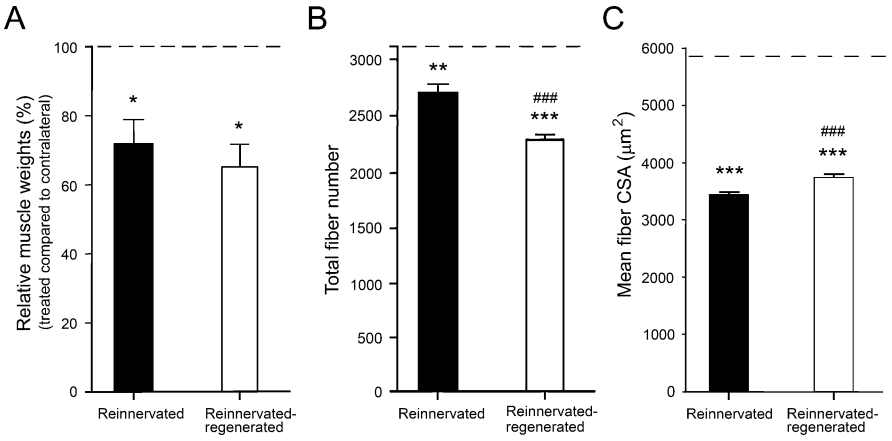

Figure 1 Relative muscle weights (**A**), total fiber number (**B**), and mean fiber cross-sectional area (CSA) (**C**) of reinnervated versus reinnervated-regenerated soleus muscles. Relative muscle weights compared with contralateral (unaffected) counterparts are shown in **A**. Contralateral muscle weights are considered as 100% (dashed line). Total fiber number and mean fiber CSA of aged-matched normal soleus (3099 ± 94 and 5886 ± 54 μm^2, respectively) are depicted as dashed lines in **B** and **C**, respectively. Bars represent mean values ± SEM, $n=3$, asterisks show significant differences compared with normal muscles (*$p<0.05$, **$p<0.01$, ***$p<0.001$), and hatches represent significant differences between reinnervated and reinnervated-regenerated muscles ($^{\#\#\#}p<0.001$). Muscle weights, fiber number, and mean fiber CSA are significantly decreased in reinnervated soleus when compared with normal soleus, and regenerated-reinnervated muscles show a further significant decrease in fiber number but an increase in mean fiber CSA when compared with reinnervated soleus.

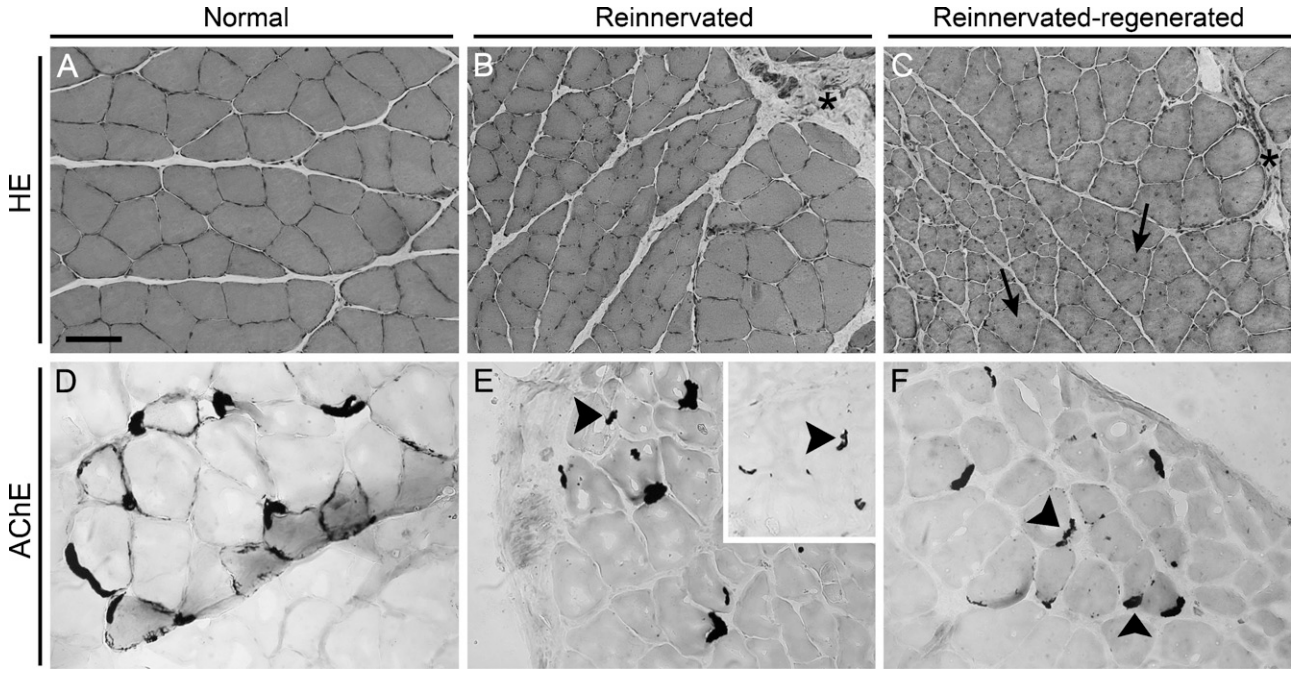

Figure 2 Morphology of the reinnervated and reinnervated-regenerated soleus muscles. Depicted are sections stained with either hematoxylin-eosin (HE) (**A–C**) or with Tago's method (for AChE activity of motor endplates) (**D–F**). Compared with normal age-matched soleus (**A,D**), reinnervated muscle fibers are atrophied to different degrees (see small and larger fibers) (**B**). Accumulation of connective tissue (**B**, asterisk) and several endplates of abnormal morphology (**E**, arrowheads; see also a different area on inset) are evident. Regenerated-reinnervated soleus is characterized by an extremely variable fiber size, with a significant number of centrally located nuclei (**C**, arrows), by abundant connective tissue (**C**, asterisk) also around fibers, and by a remarkable number of abnormal (fragmented or granular) endplates (**F**, arrowheads). Bar = 100 μm.

regeneration (Whalen et al. 1990). In the morphological sense, these data are indicative of an altered, less-synchronous, and less-effective regeneration process in reinnervated soleus. To gain information about the innervation state of the affected muscles, we performed AChE staining of motor endplates as well (Figures 2D–2F; Pintér et al. 2003). In reinnervated muscles, we confirmed the findings of others (Ijkema-Paassen et al. 2002) who found highly variable motor endplates, several of which were characterized by abnormal (fragmented or granular) morphology (Figure 2E, arrowheads; see also inset). In reinnervated-regenerated muscles (i.e., on day 28 of regeneration), we observed motor endplates with similar morphological abnormalities coupled several times to smaller fibers (Figure 2F, arrowheads; Pintér et al. 2003). To summarize, our morphometric and morphological data revealed both quantitative and qualitative alterations in the regeneration process of reinnervated-regenerated muscles when compared with reinnervated and normal ones.

MHC Composition Based on Immunohistochemical Analysis

To analyze the possible effects of reinnervation and subsequent regeneration on MHC composition, serial crysections were immunostained with a set of monoclonal antibodies to distinguish and count (pure and hybrid) fibers expressing different MHC isoforms.

Reinnervated Muscles. In contrast to normal soleus, which contains 80–90% of slow type I fibers (not shown; Delp and Duan 1996), their number dramatically decreased to ~33% after reinnervation (Figures 3A and 4A), and the amount of fast fibers significantly increased from ~10–20% to 85% (Figures 3B and 4A). Although similar data have already been published in the literature (Bodine and Pierotti 1996; Huey and Bodine 1996; Ijkema-Paassen et al. 2002), the differential immunohistochemical analysis of the MHCII isoforms has not been carried out to date. We found that most of the fast II fibers were IIA fibers (44%) (Figures 3C and 4A), and no fibers expressed the fastest MHCIIB isoform (Figures 3D and 4A). The number of pure (not hybrid) IIX fibers was estimated according to the difference between II and IIA fibers, which proved to be ~40% (Figures 3B–3D and 4A). Another notable change was the increased number (~20%) of I/II hybrid fibers expressing both slow MHCI and fast MHCII (Figures 3A–3C and 4B) compared with those in normal soleus (less than 8%; Staron et al. 1999). Most of the I/II hybrids present in reinnervated soleus seemed to express MHCIIA as the fast isoform (Figures 3A and 3C). In addition, we observed variable staining intensity of the

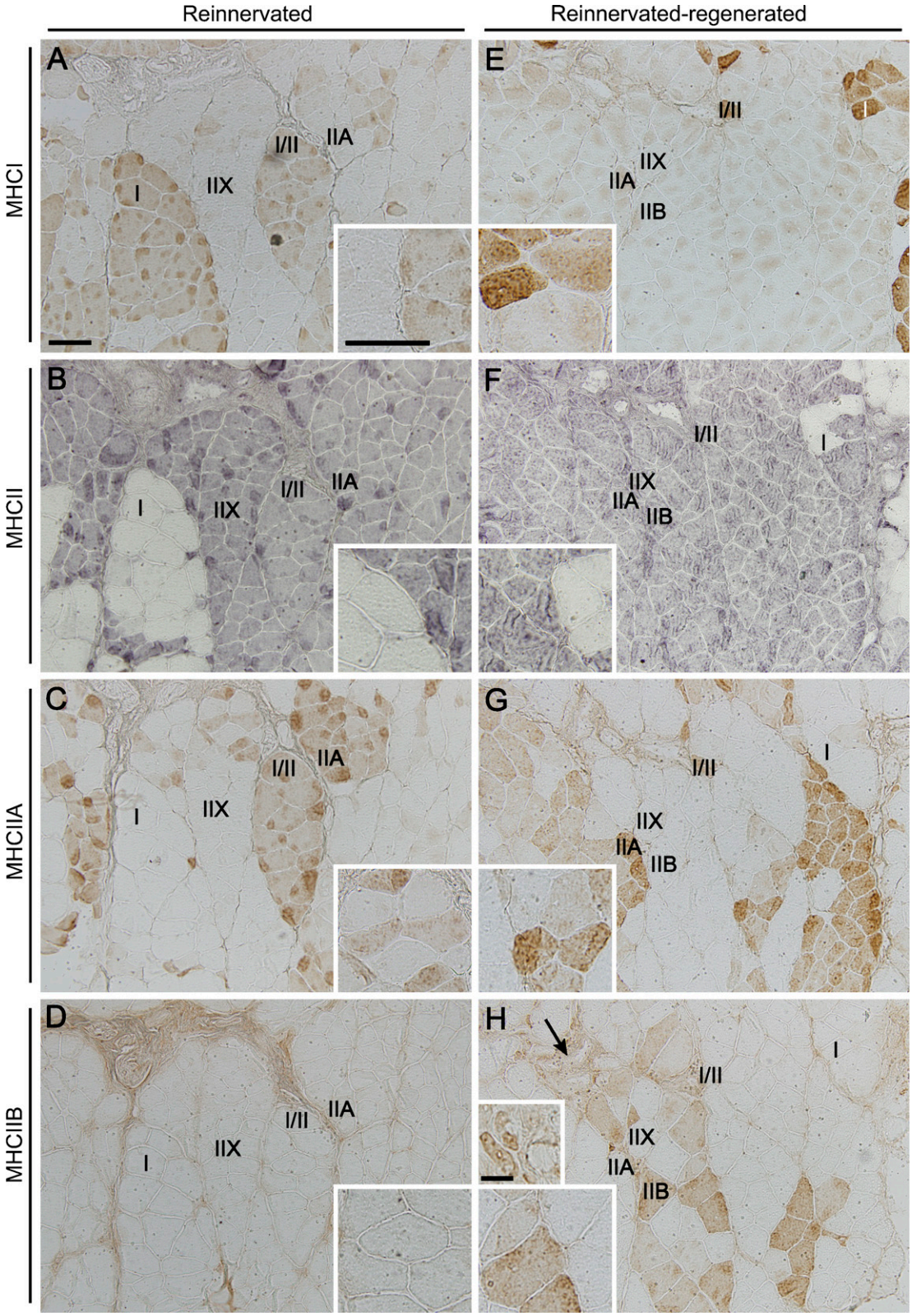

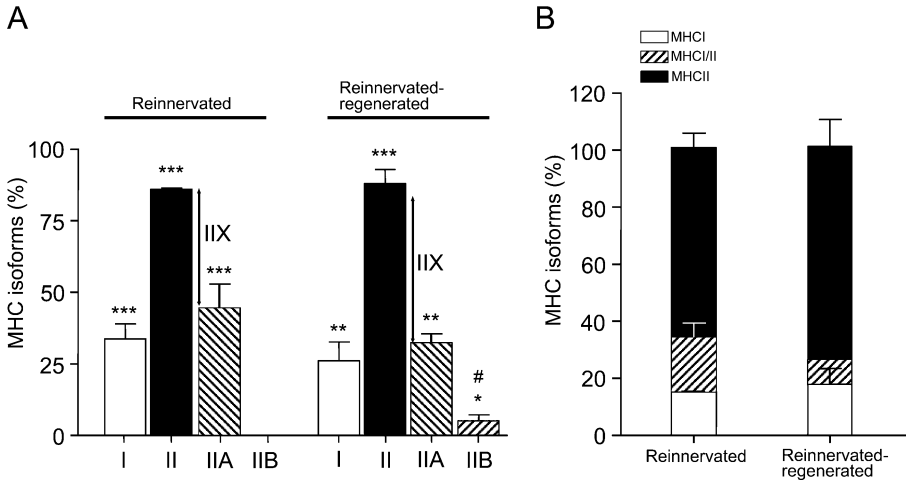

Figure 4 Fiber type distribution after reinnervation and subsequent regeneration of soleus muscle. (**A**) Bars represent the ratio (%) of MHCI-, MHCII-, MHCIIA-, and MHCIIB-expressing fibers (± SEM) in reinnervated and reinnervated-regenerated muscles, respectively (n=3–4). The estimated proportion of pure (non-hybrid) IIX fibers (calculated from the difference of type II and type IIA + IIB fibers) is indicated by an arrow in both treated groups. Total number (pure + hybrid) of IIX fibers is likely to be higher than that of the pure fibers. In reinnervated soleus, a significant drop in the number of slow type I fibers is present, accompanied by a significant increase in that of fast type II fibers (mainly IIA and IIX), compared with normal soleus (not shown). The fastest IIB fibers are not detectable. After regeneration, further slow-to-fast transition can be observed, based on the decreasing tendency of IIA fibers and a simultaneous increase of IIX fibers. A remarkable number of the fastest IIB fibers appear. Asterisks indicate significant changes compared with the respective MHC isoforms in normal soleus (Staron et al. 1999) (*p<0.05, **p<0.01, ***p<0.001), and hatch indicates a significant difference between the reinnervated and reinnervated-regenerated groups (#<0.05). (**B**) The proportions of pure type I (slow), pure type II (fast), and hybrid (I/II) fibers are shown (see bar legend). In reinnervated soleus, a high proportion (~20%) of I/II hybrid fibers is detectable, which tends to decrease after regeneration (8%), in parallel with a slight increase in pure type II (fast) fibers.

individual I/IIA hybrid fibers (Figures 3A and 3C, and insets), which may indicate a dynamic transition of type I to type IIA fibers, similar to the stepwise transformation of slow fibers toward fast ones in inactivity and cross-reinnervation studies (Pette and Vrbová 1992). Moreover, spatial grouping of the same MHC-expressing fibers was clearly detectable in all of the examined sections (Figures 3A–3C), which is a phenomenon seen after reinnervation (Ijkema-Paassen et al. 2001; Wang et al. 2002).

Reinnervated–Regenerated Muscles. As a remarkable novel finding, we observed a further slow-to-fast (i.e., oxidative-to-glycolytic) shift in the phenotype of reinnervated soleus after regeneration took place. Although the ratio of slow type I to fast type II fibers (26/88%; Figures 3E and 3F and Figure 4A) did not differ significantly from that of the reinnervated muscles, it showed a clear tendency toward a faster phenotype. Among fast fibers, the number of fast oxidative IIA fibers tended to decrease from 44% to ~32% (Figures 3G and 4A), and even the fastest glycolytic IIB isoform (undetectable in the reinnervated muscle) was expressed in a significant number of fibers after regeneration (~5%; Figures 3H and 4A). The size and staining intensity of IIB fibers was notably variable. Very small, unmatured regenerated fibers with central nuclei were found mainly in areas where muscle regeneration was less effective, surrounded by increased amounts of connective tissue (Figure 3H, arrow; compare also small and large insets). On the other hand, larger fibers expressed MHCIIB in varying intensity (Figure 3H and large inset), which indicates that IIB fibers of fainter staining might be hybrid fibers coexpressing other fast isoforms (MHCIIX) as well. The estimated number of pure IIX fibers tended to increase from 40% to ~51% (Figures 3F–3H and 4A). As further proof of a shift toward the faster phenotype, we found a relative increase in the ratio of pure fast II fibers at the expense of the number of I/II hybrid fibers, which decreased from

Figure 3 Immunohistochemical analysis of myosin heavy chain (MHC) isoforms in reinnervated versus reinnervated-regenerated soleus muscles. **A–D** represent serial sections of reinnervated muscles, and **E–H** show those of reinnervated-regenerated soleus. Insets show higher magnification of some fibers, with characteristic staining in each photograph. Antibodies against MHCI (**A,E**), MHCII (**B,F**), MHCIIA (**C,G**), and MHCIIB (**D,H**) are used. Fibers not stained for any of the above-mentioned antibodies except MHCII are considered to be IIX fibers. The same representative fibers are marked as I, IIX, IIA, IIB, and I/II hybrid fibers in the serial sections stained with different antibodies in either reinnervated (**A–D**), or reinnervated-regenerated muscles (**E–H**). Compared with the mainly slow-type normal soleus (not shown), the population of slow type I fibers is dramatically decreased after transection, followed by a 3-month period of reinnervation (**A**), and the number of fast II fibers is increased (**B**), accompanied by a significant number of I/II hybrid fibers as well (compare **A,B,C**). A remarkable number of fast type IIA (**C**) and IIX (**B,C,D**) fibers are detected, but MHCIIB-expressing fibers are not present (**D**). After a 28-day muscle regeneration, only a few MHCI-expressing fibers can be observed (**E**), because the majority of fibers are fast (**F**). In addition to IIA (**G**) and IIX (**F,G,H**) fibers, the most-glycolytic IIB fibers (**H**) are also present, characterized by variable size (arrow shows an area of connective tissue and small fibers; see also smaller inset for very small fibers) and staining intensity (see also larger inset). The proportion of I/II hybrid fibers is somewhat decreased (**E,F**). Bars: **A–H** = 100 μm; smaller inset **H** = 20 μm.

20% to ~8% (Figure 4B). Although several type II fibers were probably hybrids coexpressing different fast isoforms (MHCIIA/IIX, MHCIIX/IIB, or MHCIIA/IIX/IIB), we could not distinguish them, owing to the lack of a specific IIX antibody. To summarize our new findings, the regeneration process of the reinnervated soleus (reinnervation-regeneration model), in contrast to the uniformly slow-fiber composition of soleus muscle after normal regeneration, resulted in an even faster muscle phenotype with a notable presence of different populations of IIB fibers.

Mean Fiber CSA and Frequency Distribution of MHCI, MHCII, and MHCIIB Fibers

Because fiber size could be indicative of the innervation (atrophy) level of fibers, we aimed at analyzing whether there are different fiber populations in reinnervated-regenerated muscles compared with reinnervated ones. In normal slow-type soleus, CSAs of type I fibers were somewhat larger than those of type II fibers (5909 ± 55 μm^2 and 5295 ± 79 μm^2, respectively; Table 2; Delp and Duan 1996). In reinnervated muscles compared with normal muscles, type I fibers became smaller (4945 ± 110 μm^2; Table 2). However, the frequency distribution revealed two main populations, one with a close-to-normal CSA and the other with a remarkably smaller CSA (Figure 5A, black bars, two peaks at ~5500 μm^2 and 3000–3500 μm^2, respectively, n=318). These findings suggest that the larger fibers expressing MHCI were perfectly reinnervated by slow axons maintaining their original size, whereas smaller MHCI fibers may represent different populations, which have been either denervated but not transformed yet, or reinnervated by foreign (slow or fast) axons. Type II fibers seemed to be uniformly smaller-sized (2998 ± 31 μm^2; Table 2; Figure 5B, black bars, n=1079) with less than 9% of fibers smaller than 1750 μm^2 (Table 2; Figure 5B), indicating that most of them might be reinnervated.

Table 2 Mean fiber CSA of MHCI, MHCII and MHCIIB fibers in normal, reinnervated, and reinnervated-regenerated soleus muscles

Fiber type	Normal	Reinnervated	Reinnervated-regenerated
MHCI	5909 ± 55[a]	4945 ± 110[a,b]	3300 ± 80[a,b,c]
MHCII (all)	5295 ± 79	2998 ± 31[b]	3915 ± 75[b,c]
MHCII (>1750 μm^2)		3145 ± 29[b]	4480 ± 74[b,c]
MHCIIB (all)			3088 ± 185[a,b,c]
MHCIIB (>1750 μm^2)			5326 ± 180[a,b,c]

[a]Significant difference between MHCI and II (and IIB) fibers within the respective animal group.
[b]Significant difference compared to respective fiber type in normal muscles.
[c]Significant difference between the respective fiber types in reinnervated and reinnervated-regenerated muscles.
Values are expressed as mean ± SEM (μm^2).

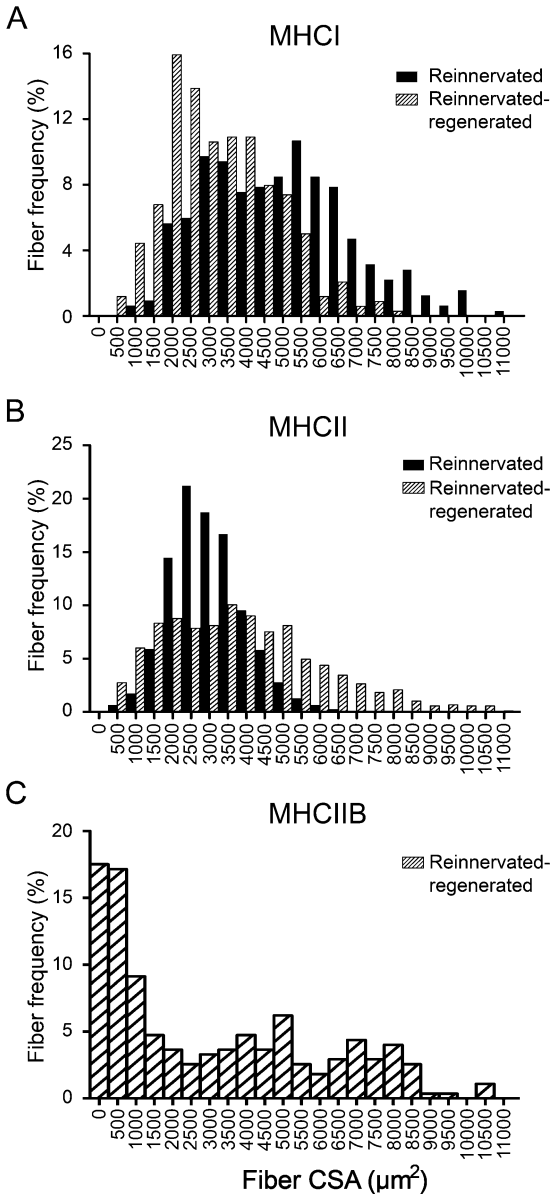

Figure 5 Frequency distribution of MHCI (**A**), MHCII (**B**), and MHCIIB (**C**) fiber CSA in reinnervated versus reinnervated-regenerated muscles. CSA of MHCI- and MHCII-expressing fibers were measured on both reinnervated and reinnervated-regenerated muscle sections stained with the sc-75 antibody, and MHCIIB fibers were analyzed on reinnervated-regenerated sections stained with the BF-F3 antibody. (**A**) MHCI fibers in reinnervated muscles (n=318) show two peaks on the histogram, representing two main fiber populations characterized by a smaller and a larger CSA, respectively, whereas in reinnervated-regenerated muscles, type I fibers (n=339) are generally smaller, with only one peak of distribution. (**B**) MHCII fibers in reinnervated muscles (n=1079) are smaller, with a narrow one-peak histogram, whereas in reinnervated-regenerated soleus (n=865), they are somewhat larger and marked by a wide distribution, starting at very small fibers on one tail and ending up in larger fibers on the other tail. (**C**) The histogram of IIB fibers in reinnervated-regenerated muscles shows that about half of the fiber population is very small (<1750 μm^2), whereas the other half is larger and distributed almost evenly between 2000–8500 μm^2.

In reinnervated-regenerated muscles, the CSA of MHCI-expressing fibers became generally smaller, characterized by only one peak of a narrow-type distribution (3300 ± 80 μm^2; Table 2; Figure 5A, hatched bars, n=339), showing that the recovery of slow fibers was impaired or delayed in the regeneration process. By contrast, MHCII fibers in reinnervated-regenerated soleus became larger than those in reinnervated soleus (3915 ± 75 μm^2; Table 2; Figure 5B, hatched bars, n=865), and also larger than the regenerated MHCI fibers (Table 2; compare Figures 5A and 5B, hatched bars). The histogram of type II fibers showed a wide distribution profile starting at very small fibers on one tail and ending up in larger fibers on the other tail. The small fibers with characteristic central nuclei (CSA <1750 μm^2) make up ~17% of type II fibers and probably represent, at least a part of them, denervated unmatured fibers not able to fully differentiate in the absence of innervation. Indeed, as revealed by the size distribution of IIB fibers in reinnervated-regenerated muscles (3088 ± 185 μm^2; Table 2; Figure 5C), about half of the fiber population was relatively small (CSA <1750 μm^2), suggesting that a notable part of the smaller type II fibers expressed MHCIIB, a default isoform in the denervated regenerated fibers (see also Figure 3H, small inset; Jerkovic et al. 1997). However, in the other half of the IIB fibers (CSA >1750 μm^2), mean fiber CSA was remarkably increased when compared with the similar population of MHCII fibers (5326 ± 180 μm^2 and 4480 ± 74 μm^2, respectively; Table 2). This interesting finding clearly indicates at least two populations of MHCIIB fibers (see also Figure 3H, small and large insets): a small one with denervation phenotype and a large one, which seems to be relatively hypertrophized compared with other type II fibers. In summary, we found in reinnervated-regenerated muscles that with the exception of the IIB-expressing small denervated fibers, fast type II fibers showed better recovery than did slow type I fibers at day 28 of regeneration, and a selective hypertrophy was seen in a certain population of IIB fibers.

mRNA Levels of MHC Isoforms Detected by RT-PCR

To determine whether the alterations detected at the level of fiber types are reflected in the mRNA level, we performed RT-PCR analysis for the different MHC isoforms in normal, reinnervated, and reinnervated-regenerated soleus. After total RNA gel electrophoresis, we used 28S rRNA as an internal control, the level of which proved to be stable in all of the examined animal groups (Figure 6A). By contrast, the mRNA levels of the

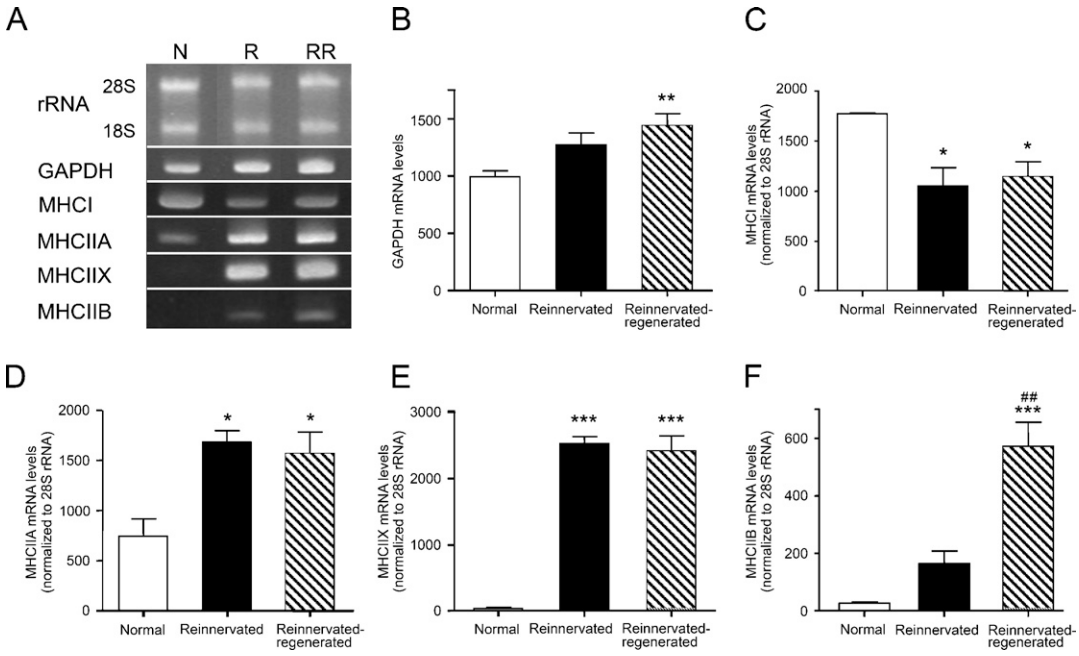

Figure 6 mRNA levels of MHC isoforms and GAPDH in normal, reinnervated, and reinnervated-regenerated soleus muscles. **A** shows representative bands of the internal control 28/18S rRNA in parallel with the characteristic amplifications for GAPDH and the different MHC isoforms. N, normal; R, reinnervated; RR, reinnervated-regenerated. Bars in **B–F** represent relative mRNA levels (mean ± SEM) normalized to 28S rRNA, except bars in **B** (n=3–5). The significant increase in the GAPDH transcript levels after regeneration (**B**) implies a glycolytic shift in the metabolism of the treated muscles. The level of slow MHCI mRNA significantly decreases as a result of reinnervation and subsequent regeneration (**C**), whereas MHCIIA (**D**) and IIX (**E**) levels are significantly increased in both treated groups, compared with normal animals. The level of MHCIIB mRNAs seems to be elevated in reinnervated soleus (p=0.05), and a further significant increase is observed in reinnervated-regenerated muscles (**F**). Asterisks show significant changes compared with normal controls (*p<0.05, **p<0.01, ***p<0.001), and hatches indicate a significant difference between reinnervated and reinnervated-regenerated muscles ($^{\#\#}p$<0.01).

glycolytic enzyme GAPDH, another internal control candidate, increased significantly after regeneration, indicating a glycolytic shift in the metabolism of the treated muscles (Figures 6A and 6B). In normal soleus, MHCI is known to be the predominant form; however, a significant decrease took place after reinnervation and subsequent regeneration (Figures 6A and 6C). In contrast, MHCIIA mRNA levels increased significantly with both treatments, compared with normal rats (Figures 6A and 6D), and a similar significant increase in MHCIIX expression was also observed in each treated group (Figures 6A and 6E). In contrast with the immunohistochemical alterations, no significant difference in MHCIIA or MHCIIX mRNA levels was found in the reinnervated versus reinnervated-regenerated groups, which is reasonable if one takes into account that total RNA was isolated from a whole muscle instead of performing single-fiber analysis. However, in accordance with immunohistochemical results, MHCIIB transcript levels were virtually not detectable in normal soleus, but a clear elevation ($p=0.05$) was seen in reinnervated muscles and a further highly significant increase took place in reinnervated-regenerated soleus (Figures 6A and 6F). These findings suggest that IIB fibers could be detectable with immunohistochemistry (in reinnervated-regenerated soleus) only when MHCIIB transcript levels were significantly elevated, whereas MHCIIB protein expression could not be visualized in individual fibers when the transcript levels were lower (in normal and reinnervated soleus). Our results are in agreement with the predominant transcriptional regulation of MHC isoforms described in slow-type skeletal muscle under several conditions (Schiaffino and Reggiani 1996; Baldwin and Haddad 2001; Pandorf et al. 2006).

Discussion

The functional impairment of skeletal muscles after nerve injury, despite optimized surgery, is an intriguing medical problem (Mackinnon and Dellon 1988). We hypothesized that in addition to several reinnervation disturbances, the regenerative capacity of the reinnervated muscle is also altered, as indicated previously by morphological and motor endplate abnormalities (Pintér et al. 2003). Indeed, here we provide evidence that fiber type composition of the reinnervated-regenerated rat soleus muscle is faster than that we observed in reinnervated soleus. This finding suggests that the (fast) pattern of reinnervation plays a dominant role in the specification of fiber phenotype during regeneration, which can also contribute to the long-lasting functional impairment of the reinnervated muscle. Moreover, because the fast II fibers (and selectively, a certain population of the fast IIB fibers) showed better recovery (larger CSA) than did slow type I fibers, the faster phenotype of the reinnervated-regenerated muscle seems to be actively maintained by selective yet undefined cues.

We applied a rat model of sciatic nerve transection and immediate repair by graft to analyze the regenerative machinery of reinnervated muscles (Pintér et al. 2003). In reinnervated soleus, our previous morphological findings, as well as the present results on the slow-to-fast fiber type transition, were consistent with those of another group (Ijkema-Paassen et al. 2001), who used a very similar rat model and described time-dependent abnormalities without a significant improvement in muscle recovery, even after 60 weeks of reinnervation (Ijkema-Paassen et al. 2005). In the present study, however, we performed a more detailed analysis of the slow, hybrid, and fast fibers at both immunohistochemical and mRNA levels, examining also the size (atrophy state) of the different fiber populations, because these data are necessary for judging the reinnervation level of fibers before the induction of regeneration. Our new results, namely the significantly high number of I/II hybrids, as well as the increase in the number of both MHCIIA- or MHCIIX-expressing fibers, accompanied by respective changes in their mRNA levels, suggest a gradual slow-to-fast fiber switch in reinnervated soleus, which is regulated predominantly at the mRNA level (Schiaffino and Reggiani 1996; Baldwin and Haddad 2001; Pandorf et al. 2006).

The explanation for fiber type transition in reinnervated soleus might be either the partial denervation of certain fiber populations because of axon loss (Mackinnon et al. 1991; Lloyd et al. 2007) and/or the random reinnervation of muscles by axons of different motoneuron pools (Bodine-Fowler et al. 1997; Gramsbergen et al. 2000; Ijkema-Paassen et al. 2001). In accordance with the literature (Ijkema-Paassen et al. 2001), we found that the total fiber number significantly decreased in reinnervated soleus when compared with normal soleus, which suggests that at least one population of denervated fibers, delayed in reinnervation, has been eliminated. However, the question remains: do all denervated fibers undergo complete elimination (by apoptosis or other mechanisms); are they replaced by new myofibers originating from proliferating satellite cells to some extent; or alternatively, do they exist for a longer time in the denervated stage (Tews et al. 1997; Borisov and Carlson 2000; Borisov et al. 2001,2005; Tews 2002). In fact, Patterson et al. (2006) did not find any decrease in fiber number after 50-day denervation of rat soleus muscle, or any sign of the presence of regenerating fibers. On the basis of their findings, denervated fibers may exist for a longer time, expressing mainly fast MHC isoforms and forming several I/II hybrid fibers. However, we suggest that only a small proportion of fibers was still denervated 3 months after repair, as revealed by the difference in

muscle weights and fiber diameter of denervated versus reinnervated soleus (Pintér et al. 2003), by the relatively small number of very small fibers in reinnervated muscles, and by the notably high proportion of muscle fibers recovering from notexin-induced necrosis. Thus, random reinnervation and the respective muscle activity pattern is a more likely explanation for fiber type and size transitions detected in reinnervated soleus (Bodine-Fowler et al. 1997; Gramsbergen et al. 2000; Ijkema-Paassen et al. 2002). It has been reported that only 14% of the original (slow) soleus motoneurons find their correct target following nerve repair, indicating that most of the reinnervating axons come from different motoneuron pools (Bodine-Fowler et al. 1997). In fact, slow fibers of normal soleus are remarkably larger than those of other hindlimb muscles and are also larger than most fast fibers, except IIB fibers (Delp and Duan 1996). We described here two populations of slow fibers, the larger one probably reinnervated by the original slow axons, and the smaller one, in which fibers may represent either denervated fibers on the way to transformation, or fibers reinnervated by foreign slow or (mismatched) fast axons. These mechanisms may even explain our results on the increased number of I/II hybrid fibers, a fiber pool that may match the one found to be polyneurally innervated in a similar animal model (Ijkema-Paassen et al. 2002). Similarly, the smaller yet remarkably uniform population of fast II fibers seems to be the consequence of a gradual fast transformation maintained by foreign axons reinnervating the soleus muscle. However, we could not detect the fastest IIB fibers in the reinnervated soleus. The reason might be that 3 months of reinnervation was not enough for a complete MHCI–MHCIIB fiber conversion and even longer reinnervation time would be required for this process (Ijkema-Paassen et al. 2001,2005). On the other hand, even if not all the fast fibers were reinnervated, it seems that denervation does not favor the expression of those fast isoforms that are not present originally in the affected muscle, like the IIB fibers in soleus (Patterson et al. 2006).

Intriguingly, reinnervated fast-type muscles, in contrast with slow-type soleus, almost regained their normal phenotype after a transient change toward the slow character (Ijkema-Paassen et al. 2001; Wang et al. 2002; Zhou et al. 2006). The different reactions of slow- and fast-type muscles upon reinnervation may be explained by their different functions, because soleus is more dependent on the amount of mechanical activity (force generation), compared with fast-type muscles (Ohira et al. 2006). On the other hand, a few data support the hypothesis that the intrinsic (innervation-independent) properties of a particular muscle, e.g., different satellite cell populations and their functions, play a major role in the specification of fiber type, even after the removal of neural input (Patterson et al. 2006). If this is the case, alterations of the muscle regenerative capacity, influenced by both intrinsic and innervation-dependent mechanisms, can also contribute to the impaired phenotype of the reinnervated soleus.

The main question of our study was whether the regenerative machinery of the reinnervated soleus can reproduce the original muscle phenotype in both qualitative and quantitative senses. In the present study, we clarified that the total fiber number was significantly lower after 28 days of regeneration in reinnervated-regenerated muscles, compared with reinnervated ones. The “missing” fibers may represent a fiber population in reinnervated muscles that has not been properly reinnervated and that therefore could not maintain the subsequent growth of regenerated fibers. Otherwise, the mean fiber CSA of the existing fibers was even larger in the reinnervated-regenerated muscles than that in the reinnervated soleus (but smaller than that in normal soleus), indicating that the recovery of certain fiber populations was preferred after regeneration. Indeed, we detected here that even though slow-type regenerating fibers did not reach the size characteristic of those in reinnervated soleus, fast fibers were generally larger in reinnervated-regenerated soleus, compared with reinnervated muscles. Moreover, a clear transition toward a faster phenotype was observed, and even the fastest IIB fibers were present after regeneration. Because no reverse change occurred toward a slower phenotype even by day 35 (data not shown), it is unlikely that all these abnormalities are simple consequences of a delayed regeneration process resulting from additional innervation problems. Although notexin destroys motor endplates, several endplates were re-established at their original sites in both normally innervated and reinnervated soleus by day 5, and the axons seemed to recover by the end of regeneration (Harris et al. 2000; Pintér et al. 2003). Accordingly, the axon population reinnervating the soleus muscle after nerve repair should be essentially the same even after necrosis and subsequent regeneration.

Therefore, other explanations should exist for the phenotype shift accompanied by the appearance of IIB fibers during the regeneration process. In fact, it is the MHCIIB and IIX mRNAs and proteins that are expressed in the first few days of normal regeneration, at the time when destroyed motor endplates have not yet been re-established. After the recovery of motor endplates and slow-type innervation, both MHCIIX and IIB mRNAs and proteins decrease gradually in parallel with the increase in slow-type MHCI expression. In accordance with these data, denervated slow-type soleus expressed exclusively the fast MHCIIX and IIB mRNAs in the regeneration process (Esser et al. 1993; Jerkovic et al. 1997). Other reports also suggest

that IIB fibers develop in the absence of neural stimulation (Butler-Browne et al. 1982; Schiaffino and Reggiani 1996; Fink et al. 2003). Thus, the relatively small MHCIIB-expressing fibers, often located in the connective tissue–rich areas in our experiments, certainly represent denervated fibers that could not accomplish MHC transitions and growth. However, the larger part of the MHCII-expressing fibers, and especially about half of the IIB fibers, reached a significantly larger size after regeneration, suggesting an active (fast-type) innervation of them. Thus, our results regarding fast-fiber transition can be interpreted as the impairment of the physiological fast-to-slow conversion during the regeneration process either due to denervation (small II and IIB fibers) or mainly, due to active maintenance of the (larger) fast fibers at the expense of the (smaller) slow ones. The latter finding is intriguing, particularly because it is the slow-fiber population that becomes dominant in normal soleus muscle regenerating from notexin-induced necrosis (Whalen et al. 1990). It cannot be ruled out that intrinsic muscle characteristics, such as a subpopulation of satellite cells determined to produce mainly slow-type or oxidative fibers (Kalhovde et al. 2005), are selectively impaired in reinnervated soleus, which in turn hampers the proper reaction to slow-type innervation, causing a delayed regeneration. This possibility might be tested in additional experiments at later stages of regeneration (i.e., several weeks after notexin treatment) to see whether the difference in the size of slow versus fast fibers would be still apparent. Another explanation for size differences might be that because of different cues, fast-type axons or their collaterals become more effective in reinnervated-regenerated muscles than do slow-type ones. Some recent reports have shown a definite role of active (fast-type) innervation in the expression of the MHCIIB isoform (Di Maso et al. 2000; Germinario et al. 2002). Moreover, from the view of several neurotrophic factors influencing peripheral nerve regeneration, neurotrophin-3 and neurotrophin-4 have been described to favor selectively the axon regeneration of fast (IIB) and slow motoneuron pools, respectively, playing an important role in determining the correct muscle phenotype (Sterne et al. 1997; Kingham and Terenghi 2006). Further investigations are needed to explore the significance of neurotrophins, especially of neurotrophin-3 in supporting the recovery of fast IIB (and II) fibers in the altered regeneration of the reinnervated soleus.

In conclusion, the morphological, fiber type, and size alterations detected in reinnervated-regenerated soleus could be the consequence of a complex process involving both innervation-dependent and/or -independent molecular mechanisms, the exploration of which may contribute to a more effective therapy for the functionally impaired reinnervated muscle.

Acknowledgments

This work was supported by grants from Medical Scientific Board, Hungary (ETT) 421/2003, ETT 008/2006, and Regional Science Center of the University of Szeged, Hungary (RET) 08/2004 National Technological Development Board, Hungary (OMFB)-0066/2005. We thank Balásházi Istvánné for the technical assistance in animal experiments.

Literature Cited

Baldwin KM, Haddad F (2001) Effects of different activity and inactivity paradigms on myosin heavy chain gene expression in striated muscle. J Appl Physiol 90:345–357

Bischoff R (1994) The satellite cell and muscle regeneration. In Engel AG, Franzini-Armstrong C., eds. Myology, vol. 1, Basic and clinical. 2nd ed. Columbus, McGraw-Hill, Inc., 97–118

Bodine SC, Pierotti DJ (1996) Myosin heavy chain mRNA and protein expression in single fibers of the rat soleus following reinnervation. Neurosci Lett 215:13–16

Bodine-Fowler S, Meyer RS, Moskovitz A, Abrams R, Botte MJ (1997) Inaccurate projection of rat soleus motoneurons: a comparison of nerve repair techniques. Muscle Nerve 20:29–37

Borisov AB, Carlson BM (2000) Cell death in denervated skeletal muscle is distinct from classical apoptosis. Anat Rec 258:305–318

Borisov AB, Dedkov E, Carlson BM (2001) Interrelations of myogenic response, progressive atrophy of muscle fibers, and cell death in denervated skeletal muscle. Anat Rec 264:203–218

Borisov AB, Dedkov EI, Carlson BM (2005) Abortive myogenesis in denervated skeletal muscle: differentiative properties of satellite cells, their migration, and block of terminal differentiation. Anat Embryol (Berl) 209:269–279

Butler-Browne GS, Bugaisky LB, Cuenoud S, Schwartz K, Whalen RG (1982) Denervation of newborn rat muscle does not block the appearance of adult fast myosin heavy chain. Nature 299: 830–833

Chomczynski P, Sacchi N (1987) Single-step method of RNA isolation by acid-guanidium thiocyanate-phenol-chloroform extraction. Anal Biochem 162:156–159

Davis CE, Harris JB, Nicholson LV (1991) Myosin isoform transitions and physiological properties of regenerated and re-innervated soleus muscles of the rat. Neuromuscul Disord 1:411–421

Delp MD, Duan C (1996) Composition and size of type I, IIA, IID/X, and IIB fibers and citrate synthase activity of rat muscle. J Appl Physiol 80:261–270

Di Maso NA, Haddad F, Zeng M, McCue SA, Baldwin KM (2000) Role of denervation in modulating IIb MHC gene expression in response to T_3 plus unloading state. J Appl Physiol 88:682–689

Esser K, Gunning P, Hardeman E (1993) Nerve-dependent and–independent patterns of mRNA expression in regenerating skeletal muscle. Dev Biol 159:173–183

Fink E, Fortin D, Serrurier B, Ventura-Clapier R, Biggard AX (2003) Recovery of contractile and metabolic phenotypes in regenerating slow muscle after notexin-induced or crush injury. J Muscle Res Cell Motil 24:421–429

Germinario E, Esposito A, Megighian A, Midrio M, Biral D, Betto R, Danieli-Betto D (2002) Early changes of type 2B fibers after denervation of rat EDL skeletal muscle. J Appl Physiol 92:2045–2052

Girgenrath S, Song K, Whittemore LA (2005) Loss of myostatin expression alters fiber-type distribution and expression of myosin heavy chain isoforms in slow- and fast-type skeletal muscle. Muscle Nerve 31:34–40

Gramsbergen A, Ijkema-Paassen J, Meek MF (2000) Sciatic nerve transection in the adult rat: abnormal EMG patterns during locomotion by aberrant innervation of hindleg muscles. Exp Neurol 161:183–193

Grubb BD, Harris JB, Schofield IS (1991) Neuromuscular transmission at newly formed neuromuscular junctions in the regenerating soleus muscle of the rat. J Physiol 441:405–421

Gutmann E, Zelena J (1962) Morphological changes in the denervated muscle. In Gutmann E., ed., The Denervated Muscle. Prague,

Prague Publishing House of the Czechoslovak Academy of Sciences, 341–371
Hare GM, Evans PJ, Mackinnon SE, Best TJ, Bain JR, Szalai JP, Hunter DA (1992) Walking track analysis: a long-term assessment of peripheral nerve recovery. Plast Reconstr Surg 100:251–258
Harris JB, Grubb BD, Maltin CA, Dixon R (2000) The neurotoxicity of the venom phospholipases A_2, notexin and taipoxin. Exp Neurol 161:517–526
Harris JB, Johnson MA, Karlsson E (1975) Pathological responses of rat skeletal muscle for a single subcutaneous injection of a toxin isolated from the venom of the Australian tiger snake, Notechis scutatus scutatus. Clin Exp Pharmacol Physiol 2:383–404
Huey KA, Bodine SC (1996) Altered expression of myosin mRNA and protein in rat soleus and tibialis anterior following reinnervation. Am J Physiol 271:C2016–C2026
Ijkema-Paassen J, Meek MF, Gramsbergen A (2001) Muscle differentiation after sciatic nerve transection and reinnervation in adult rats. Ann Anat 183:369–377
Ijkema-Paassen J, Meek MF, Gramsbergen A (2002) Reinnervation of muscles after transection of the sciatic nerve in adult rats. Muscle Nerve 25:891–897
Ijkema-Paassen J, Meek MF, Gramsbergen A (2005) Long-term reinnervation effects after sciatic nerve lesions in adult rats. Ann Anat 187:113–120
Jaschinski F, Schuler M, Peuker H, Pette D (1998) Changes in myosin heavy chain mRNA and protein levels of rat muscle during forced contractile activity. Am J Physiol 274:C365–370
Jerkovic R, Argentini C, Serrano-Sanchez A, Cordonnier C, Calabria E, Schiaffino S, Lomo T (1997) Early myosin switching induced by nerve activity in regenerating slow skeletal muscle. Cell Struct Funct 22:147–153
Kalhovde JM, Jerkovic R, Sefland I, Cordonnier C, Calabria E, Schiaffino S, Lomo T (2005) "Fast" and "slow" muscle fibers in hindlimb muscles of adult rats regenerate from intrinsically different satellite cells. J Physiol 562:847–857
Kalliainen LK, Jejurikar SS, Liang LW, Urbanchek MG, Kuzon WM (2002) A specific force deficit exists in skeletal muscle after partial denervation. Muscle Nerve 25:31–38
Kingham PJ, Terenghi G (2006) Bioengineered nerve regeneration and muscle reinnervation. J Anat 209:511–526
Lefaucheur JP, Sebille A (1995) The cellular events of injured muscle regeneration depend on the nature of the injury. Neuromuscul Disord 5:501–509
Lloyd BM, Luginbuhl RD, Brenner MJ, Rocque BG, Tung TH, Myckatyn TM, Hunter DA, et al. (2007) Use of motor nerve material in peripheral nerve repair with conduits. Microsurgery 27: 138–145
Mackinnon SE, Dellon AL (1988) Surgery of the Peripheral Nerve. New York, Thieme
Mackinnon SE, Dellon AL, O'Brien JP (1991) Changes in nerve fiber numbers distal to a nerve repair in the rat sciatic nerve model. Muscle Nerve 14:1116–1122
Mendler L, Szakonyi G, Zádor E, Görbe A, Dux L, Wuytack F (1998) Expression of sarcoplasmic/endoplasmic reticulum Ca^{2+} ATPases in the rat extensor digitorum longus (EDL) muscle regenerating from notexin-induced necrosis. J Muscle Res Cell Motil 19:777–785
Mendler L, Zádor E, Ver Heyen M, Dux L, Wuytack F (2000) Myostatin in regenerating rat muscles and in myogenic cell cultures. J Muscle Res Cell Motil 21:551–563
Ohira Y, Yoshinaga T, Ohara M, Kawano F, Wang XD, Higo Y, Terada M, et al. (2006) The role of neural and mechanical influences in maintaining normal fast and slow muscle properties. Cells Tissues Organs 182:129–142
Pandorf CE, Haddad F, Roy RR, Qin AX, Edgerton VR, Baldwin KM (2006) Dynamics of myosin heavy chain gene regulation in slow skeletal muscle. J Biol Chem 281:38330–38342
Patterson MF, Stephenson GMM, Stephenson DG (2006) Denervation produces different single fiber phenotypes in fast- and slow-twitch hindlimb muscles of the rat. Am J Physiol Cell Physiol 291:518–528
Pette D, Staron R (1990) Cellular and molecular diversities of mammalian skeletal muscle fibers. Rev Physiol Biochem Pharmacol 116:1–76
Pette D, Vrbová G (1992) Adaptation of mammalian skeletal muscle fibers to chronic electrical stimulation. Rev Physiol Biochem Pharmacol 120:116–202
Pintér S, Mendler L, Dux L (2003) Neural impacts on the regeneration of skeletal muscles. Acta Biochim Pol 50:1229–1237
Schiaffino S, Gorza L, Sartore S, Saggin L, Ausoni S, Vianello M, Gundersen K, et al. (1989) Three myosin heavy chain isoforms in type 2 skeletal muscle fibres. J Muscle Res Cell Motil 10: 197–205
Schiaffino S, Reggiani C (1996) Molecular diversity of myofibrillar proteins: gene regulation and functional significance. Physiol Rev 76:371–424
Sesodia S, Cullen MJ (1991) The effect of denervation on the morphology of regenerating rat soleus muscles. Acta Neuropathol (Berl) 82:21–32
Staron RS, Kraemer WJ, Hikida RS, Fry AC, Murray JD, Campos GER (1999) Fiber type composition of four hindlimb muscles of adult Fisher 344 rats. Histochem Cell Biol 111:117–123
Sterne GD, Coulton GR, Browb RA, Green CJ, Terenghi G (1997) Neurotrophin-3-enhanced nerve regeneration selectively improves recovery of muscle fibers expressing myosin heavy chains 2b. J Cell Biol 139:709–715
Tago H, Kimura H, Maeda T (1986) Visualization of detailed acetylcholinesterase: fiber and neuron staining in rat brain by a sensitive histochemical procedure. J Histochem Cytochem 34: 1431–1438
Tews DS (2002) Apoptosis and muscle fibre loss in neuromuscular disorders. Neuromuscul Disord 12:613–622
Tews DS, Goebel HH, Scheider I, Gunkel A, Stennert E, Neiss WF (1997) DNA-fragmentation and expression of apoptosis-related proteins in experimentally denervated and reinnervated rat facial muscle. Neuropathol Appl Neurobiol 23:141–149
Vrbová G, Gordon T, Jones R (1995) Nerve-muscle Interaction. London, Chapman&Hall
Wang L, Copray S, Brouwer N, Meek M, Kernell D (2002) Regional distribution of slow-twitch muscle fibers after reinnervation in adult rat hindlimb muscles. Muscle Nerve 25:805–815
Whalen RG, Harris JB, Butler-Browne GS, Sesodia S (1990) Expression of myosin isoforms during notexin-induced regeneration of rat soleus muscles. Dev Biol 141:24–40
Zádor E, Mendler L, Ver Heyen M, Dux L, Wuytack F (1996) Changes in mRNA levels of the sarcoplasmic/endoplasmic-reticulum Ca2+-ATPase isoforms in the rat soleus muscle regenerating from notexin-induced necrosis. Biochem J 320:107–113
Zhou Z, Cornelius CP, Eichner M, Bornemann A (2006) Reinnervation-induced alterations in rat skeletal muscle. Neurobiol Dis 23:595–602

The Journal of Histochemistry & Cytochemistry